The 2013 World Congress on
Advances in Structural Engineering and Mechanics (ASEM13)
Jeju, Korea, September 8-12, 2013

Finite element analysis on concrete-encased CFST stub columns

*Yu-Feng An[1)], Lin-Hai Han [2)] and Xiao-Ling Zhao[3)]

1), 2) Department of Civil Engineering, Tsinghua University, Beijing, China.
3) Department of Civil Engineering, Monash University, Victoria 3800, Australia
(National "1000-Talent" Chair Professor at Tsinghua University)

1)yufeng8710@sina.com

Abstract

This paper studies the behavior of concrete-encased CFST (concrete filled steel tube) stub columns under axial compression. A finite element analysis (FEA) modeling is developed to analyze the behavior of the composite columns. Existing test data are used to verify the FEA modeling. Then full range analysis on the load versus deformation relations of the concrete-encased CFST stub columns is presented using the FEA modeling. The contributions of the inner CFST in the concrete-encased CFST stub columns is quantified.

1.Introduction

Concrete filled steel tube (CFST) can be encased in outer reinforced concrete to form an innovative type of steel-concrete composite section, named as concrete-encased concrete filled steel tube (CFST). This type of composite members has an increasing trend in being used in high-rise building and bridge structures in China. Compared to the conventional CFST columns, concrete-encased CFST columns have higher fire resistance and better durability under corrosive environment due to the protection from the outer concrete of the CFST. Concrete-encased CFST columns have easier connections with RC beams since longitudinal bars in RC beams can pass through or be anchored in the outer concrete of the CFST. Furthermore, due to the confinement provided by its outside RC, the outward buckling of the steel tube could be restrained effectively. Concrete-encased CFST columns have higher ductility due to the existence of CFST compared to conventional reinforced concrete (RC) columns (Han et al., 2009). The column section size of concrete-encased CFST columns could also be reduced by adopting high strength concrete and thin-walled high strength steel tube in CFST.

Fig.1 (a) and (b) give a schematic view of concrete-encased CFST columns during construction, as well as the typical section, respectively. It can be seen that the

1) PHD Student
2) Professor
3) Professor

concrete-encased CFST cross-section can be divided into two parts generally, i.e. the inside CFST component and the outside reinforced concrete (RC) component. The concrete outside the hooping is called “outer un-confined concrete”, whereas the concrete in between the hooping and the steel tube is called “outer confined concrete” (see Fig.1 (b)).

Some previous experimental research on concrete-encased CFST columns has been done by Chen (2002), Han et al. (2009), Kang (2009), Li et al. (2012), Liu (2013), Nie et al. (2008). However, no nonlinear 3-D finite element model was found in the literature to analyze the behavior of concrete-encased CFST columns. This paper is thus an attempt to study the compressive behavior of concrete-encased CFST stub columns. A 3-D finite element analysis model (FEA) of concrete-encased CFST stub columns under axial compression is developed and verified by test results reported previously. The complete load versus deformation relation of concrete-encased CFST stub columns is presented.

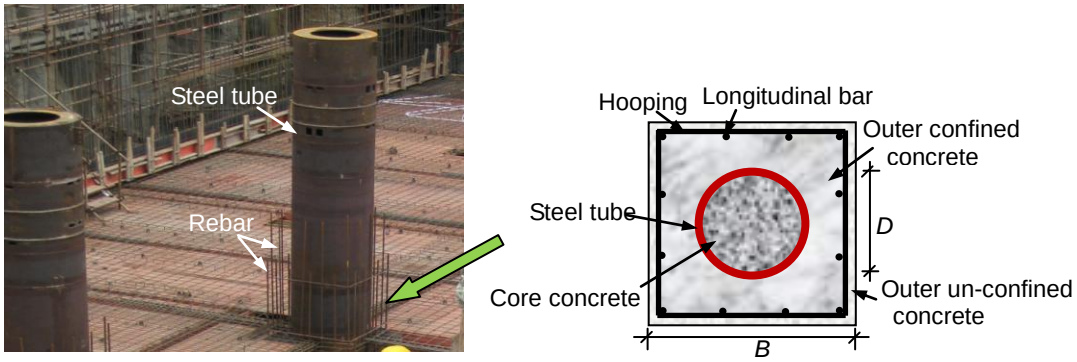

(a) During construction (b) Typical cross section

Fig.1 Concrete-encased CFST column

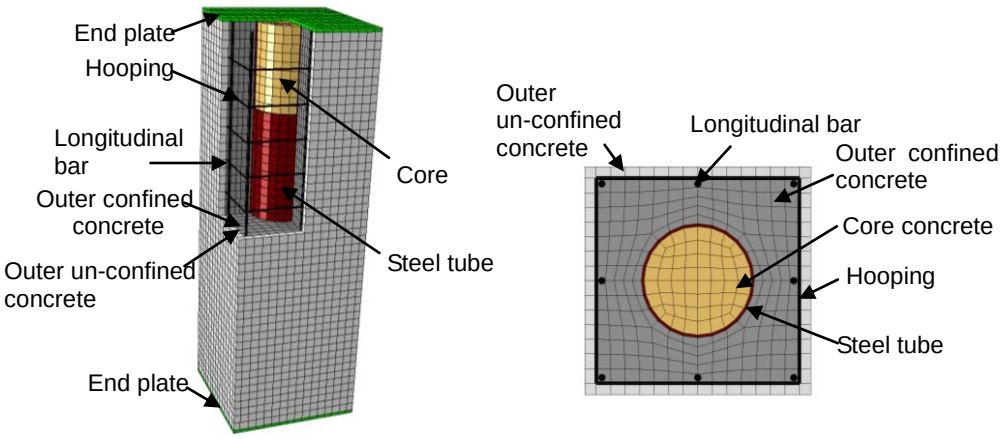

(a) Schematic view (b) Cross section

Fig. 2 Finite element model of concrete-encased CFST column

2. Finite element analysis (FEA) modeling

The analysis is conducted based on the FEA package, ABAQUS/Standard module (Hibbitt et al., 2005). Fig.2 shows a schematic view of the FEA modeling of the concrete-encased CFST column.

2.1 Material models

Elastic-plastic model is used to describe the constitutive behavior of steel, which assumes that the steel has isotropic hardening behavior. A five-stage stress-strain model illustrated for the analysis of CFST members in Han et al. (2007) is used to represent the uniaxial stress-strain relation of steel tube. The stress-strain model considering the strain hardening effect presented in Zhao et al. (2012) is used to represent the uniaxial stress-strain relation of rebar. Elastic modulus and Poisson's ratio for steel are taken as 206,000 N/mm^2 and 0.3, respectively.

Damage plasticity model is used to describe the constitutive behavior of the concrete. The elastic modulus of concrete (E_c) is taken as $4700\sqrt{f_c'}$ according to ACI 38-11 (2011), where fc' is the concrete cylinder compressive strength (in N/mm^2). Poisson's ratio is taken as 0.2. A fracture energy model suggested and described by Hillerborg et al. (1976) is used to simulate the concrete tensile softening behavior.

As shown in Fig.2 (b), the concrete across the composite section can be divided into three zones, i.e., outer un-confined concrete, outer confined concrete and core concrete of CFST according to the different confined conditions. The same approach of dividing the concrete for steel reinforced concrete (SRC) sections according to the different confined conditions can be found in Ellobody and Young (2011). A stress-strain model of unconfined concrete proposed by Attard and Setunge (1996) is applied for the uniaxial stress-strain relation of outer un-confined concrete. The detail description of the stress-strain model can be found in Attard and Setunge (1996). The strength and the plasticity of confined concrete increase compared to the unconfined concrete. In the concrete damage plasticity model the strength improvement at the state of triaxial loading can be achieved by the definition of the yielding surface. The description of the plastic behavior comes from the equivalent uniaxial stress–strain relationship. For the core concrete of CFST, the increasing of the plasticity depends on the confinement factor ξ of CFST (Han et al., 2007). A stress-strain model of core concrete in CFST provided by Han et al. (2007) is used to represent the uniaxial stress-strain relation of core concrete in concrete-encased CFST columns.

For the outer confined concrete (confinement provided by the hooping, as shown in Fig. 1b), the increasing of the plasticity mainly depends on the volumetric hooping ratio, yield stress of hooping and concrete strength. No uniaxial stress-strain model for outer confined concrete is previously available for the damage plasticity model previously. Based on the trial calculations of a large amount of testing data on hooping confined concrete stub column with square sections (as described below), a model for the uniaxial stress (σ) versus strain (ε) relation of the outer confined concrete can be defined as follows:

$$\sigma = \begin{cases} \sigma_o \dfrac{k(\varepsilon/\varepsilon_o)}{k-1+(\varepsilon/\varepsilon_o)^k} & \varepsilon \le \varepsilon_o \\ \sigma_o - E_{des}(\varepsilon - \varepsilon_o) & \varepsilon > \varepsilon_o \end{cases} \quad (1)$$

In which, $\sigma_o = f_c^{'}$; $k = \dfrac{E_c}{E_c - (\sigma_o/\varepsilon_o)}$; $\varepsilon_o = 0.00245 + 0.0122\dfrac{\rho_v f_{yh}}{f_c^{'}}$;

$E_{des} = \dfrac{0.15\sigma_0}{\varepsilon_{0.85} - \varepsilon_0}$; $\varepsilon_{0.85} = 0.225\rho_v\sqrt{\dfrac{B_c}{s}} + \varepsilon_o$;

ρ_v is the volumetric hooping ratio, f_{yh} is the yield stress of hooping, s is the hooping space, B_c is the sectional width of confined concrete.

The above strain-stress model (Eq.1) for the outer confined concrete has two characteristics compared to that of unconfined concrete: first, the strain corresponding to the maximum stress increases; and second, the descending branch of the stress–strain curves tends to have a constant slope. Fig.3 shows the above typical uniaxial stress-strain relation of outer confined concrete. In this curve, the ascend part (OA) is provided by Popovics (1973), and the descend part (A-B-C) is idealized here by a straight line. In this model, the strain (ε_o) corresponding to the maximum stress is provided by Hoshikuma et al. (1997), which is based on hooping confined concrete stub column testing data and considered the influence of the volumetric hooping ratio, yield stress of hooping and concrete strength on ε_o. The deterioration rate (E_{des}) is developed by the two points, i.e. Point A where the stress reaches the maximum, and Point B where the stress decreases to 85% of the maximum. The strain corresponding to 85% of the maximum stress ($\varepsilon_{0.85}$) is provided by Sheikh and Uzumeri (1982), which is mainly considered the influence of the volumetric hooping ratio, sectional width and hooping space, and has been verified by hooping confined concrete stub column testing data.

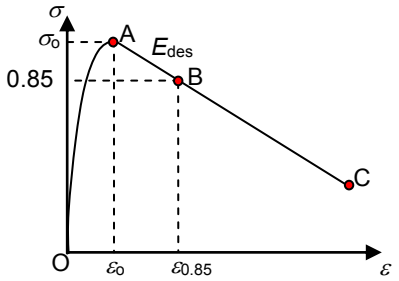

Fig. 3 Typical σ-ε relationship of confined outer concrete

2.2 Element type, mesh and boundary conditions

The end plates and concrete components including outer un-confined concrete, outer confined concrete, and core concrete of CFST are simulated by eight-node 3-D solid element with reduced integration. The steel tube is simulated by four-node conventional shell element. The rebars are simulated by using 2-node truss elements. The rebar elements are connected to outer concrete using the embedded element technique, where the translational degrees of freedom at the rebar node are eliminated. Papanikolaou and Kappos (2009) used the same approach on the rebar model and concluded that the use of truss elements was generally adequate for confinement modeling. Different grid sizes are attempted to determine an appropriate mesh. The appropriate mesh is shown in Fig.2.

The end plate is assumed to be elastic rigid block and the stiffness is large enough that the deformation in the whole loading can be neglected. The contact between the end plate and concrete components is “Hard contact”, and “Tie” is used for the contact between the end plate and steel tube, which ensure the displacements and rotational angles of the contact elements keep the same. The load is simulated by applying displacement on the end plate along the column.

2.3 Concrete and steel tube interface model

“Hard contact” is used in the normal direction between steel tube and concrete including core and outer concrete. This property can be described that there is no contact pressure unless one surface contacts another. The contact surfaces are allowed to separate each other after they have contacted. The Mohr-Coulomb friction model is applied in the tangential direction for the contact between steel tube and core concrete of CFST as described in Han et al. (2007). Up to now, there is no research reported regarding the bond behavior between steel tube and outer concrete in concrete-encased CFST columns. While as Huang et al. (2010) concluded that the behavior of concrete filled double skin steel tubular (CFDST) stub columns is not sensitive to the bond between the concrete and the inner or outer steel tube since the three components are loaded together. The bond model used for conventional CFST columns is used in CFDST columns in Huang et al. (2010). Therefore, the bond model of steel tube and core concrete is adopted for the modeling the contact between steel tube and outer concrete.

2.4 Verification of the FEA modeling

Thirty six testing specimens of concrete-encased CFST stub columns reported by Chen (2002), Kang (2009), Liu (2013) and Nie et al. (2008) are used for verification. Fig.4 gives the comparison of typical failure modes between predicted and test specimen (14-CC6). As can be seen, the outer concrete is crushed and bulges outward in the middle. The comparisons of typical predicted and measured N-ε relations of concrete-encased CFST specimens are shown in Fig.5. Fig.6 shows the comparisons of predicted N_{uc} and experimental N_{ue} of concrete-encased CFST columns. The mean value of N_{uc}/N_{ue} is 0.944, and the stand deviation is 0.076. It can be found that, in general, good agreement is obtained between the predicted and measured results.

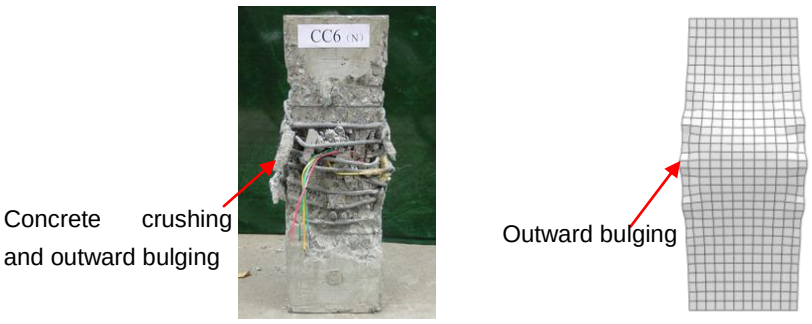

(a) Observed (Kang, 2009) (b) Predicted

Fig. 4 Comparison of failure modes between predicted and test specimen

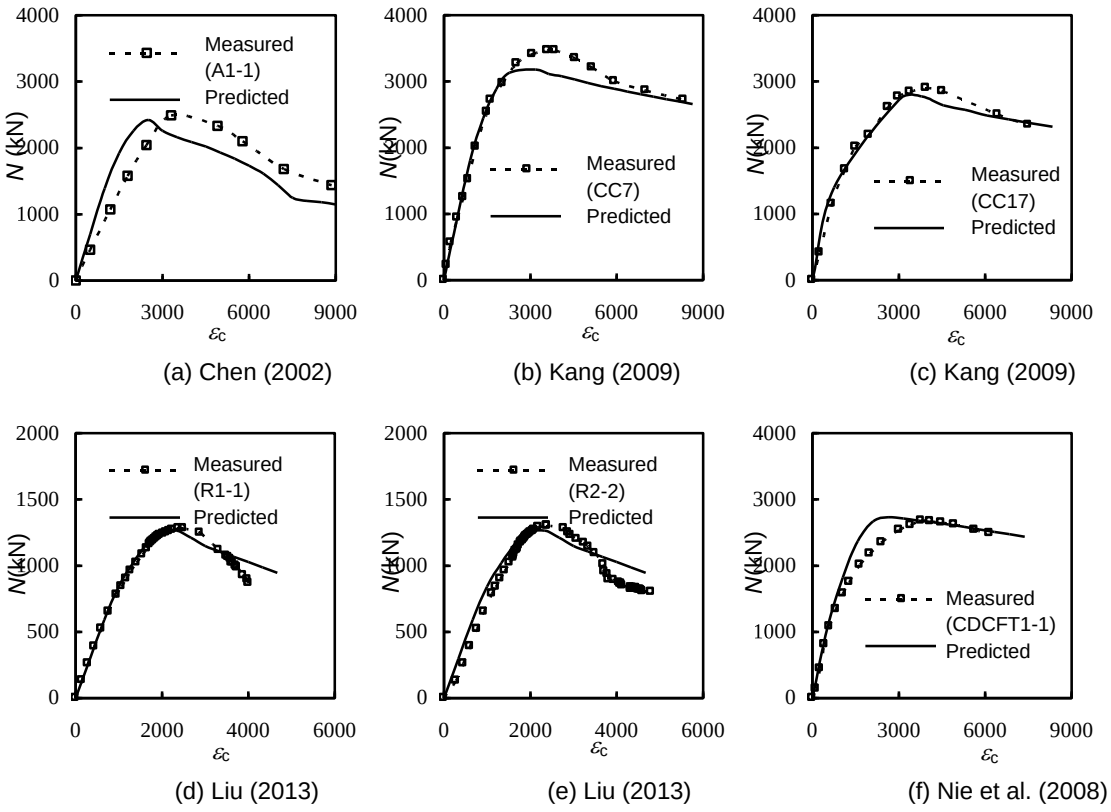

(a) Chen (2002) (b) Kang (2009) (c) Kang (2009)

(d) Liu (2013) (e) Liu (2013) (f) Nie et al. (2008)

Fig.5 N-ε relations of concrete-encased CFST specimens

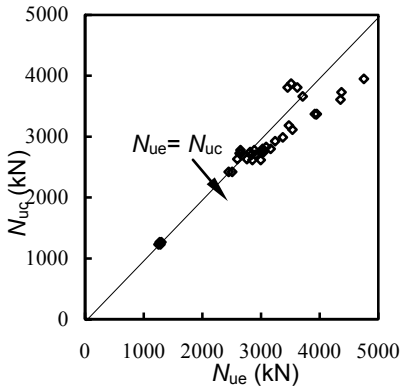

Fig. 6 Predicted N_{uc} and experimental N_{ue} of concrete-encased CFST specimens

3. Analytical behaviour

For the convenience of further investigation on the behavior of concrete-encased CFST stub columns, typical concrete-encased CFST stub column is designed. The parameters of the column are as follows: B = 400 mm, l = 1200 mm; in inner CFST component, D = 200 mm, t = 4.7 mm, f_{ys} = 345 N/mm^2, $f_{cu,core}$ = 60 N/mm^2, steel ratio of CFST α_s = 0.1; in outer RC component, $f_{cu,out}$ = 40 N/mm^2, longitudinal bar ratio α_l = 1% , f_{yl} = 345 N/mm^2, diameter of hooping is 8 mm, space s = 100 mm, f_{yh} = 235 N/mm^2, thickness of concrete cover is 20mm.

Typical calculated axial load (N) versus axial strain (ε) curve of the concrete-encased CFST column is shown in Fig.7. The axial load (N) versus axial strain (ε) curves of the components including outer un-confined concrete, outer confined concrete, core concrete of CFST, steel tube and longitudinal bar are also shown in Fig.7. Five characteristic points are marked on the curve, i.e. Point A, the steel tube begins to come into elastic-plastic stage; Point B, the outer un-confined concrete reaches the ultimate strength and begins to crush in the corners; Point C, the column reaches the ultimate strength; Point D, the load begins to be stable from descending; and Point E, the calculation is stopped due to the stability of the load. Thus, the N versus ε curve of the concrete-encased CFST column can be generally divided into five stages. The distribution of longitudinal stress of concrete in the middle of the concrete-encased CFST column at the above mentioned points is shown in Fig.8.

Stage 1: (OA). The column generally shows elastic behaviour in this stage. The stressed of outer un-confined concrete and outer confined concrete are about 80% and 65% of their peak strength, respectively. The stress of core concrete inside steel tube is about 50% of its peak strength, which is defined as the final strength when the calculation is stopped due to the stability of the load. The steel tube and longitudinal bar begin to come into elastic-plastic stage at Point A.

Stage 2: (AB). During this stage, the increasing of axial strain (ε) becomes quick with the increasing of the axial load. At Point B the outer un-confined concrete reaches the ultimate strength and begins to crush in the corners. The steel tube and longitudinal bar

has yielded at Point B. The stresses of the outer confined concrete and core concrete inside steel tube are about 95% and 70% of their peak strength, respectively.

Stage 3: (BC). The strength of the outer un-confined concrete decreases, but the strength of the column increases in this stage. At Point C the outer confined concrete reaches the ultimate strength. Though the strength of the core concrete does not decrease in the whole loading procedure, it approaches the peak value at Point C and increases slowly with the increasing of the axial strain.

Stage 4: (CD). The load begins to decrease and the axial strain increases quickly. The strengths of outer un-confined and confined concrete decrease, while the strength of core concrete increases slowly. At Point D the load begins to become stable.

Stage 5: (DE). The load keeps stable at this stage. The contribution of core concrete on the strength of the column becomes the greatest, and it is about 50% of the whole section strength.

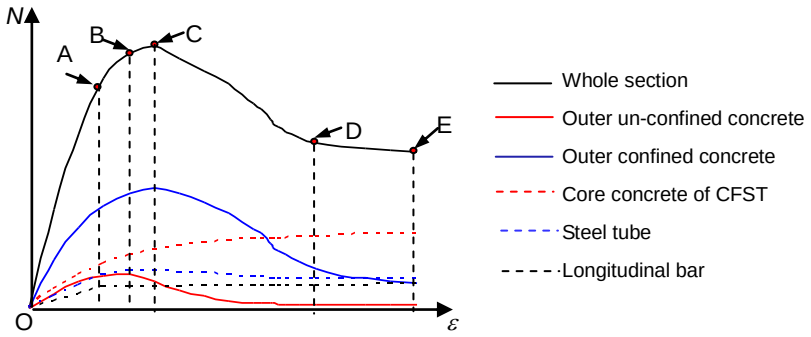

Fig. 7 Typical axial load (N) versus axial strain (ε) response

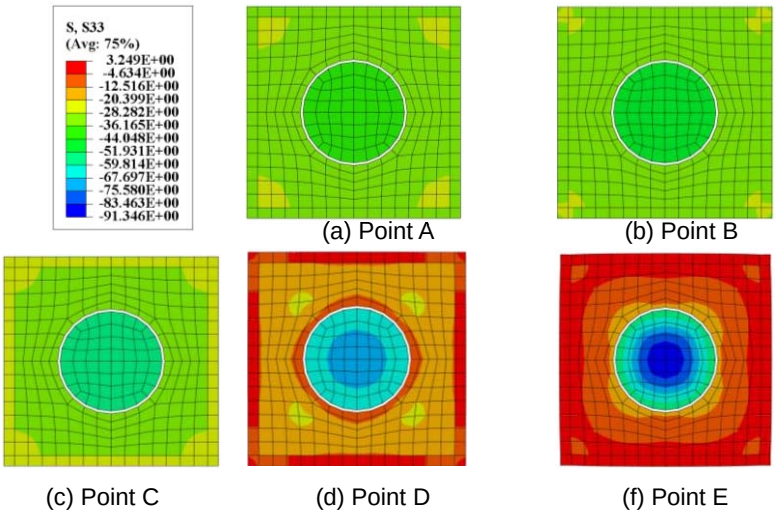

Fig.8 The distribution of longitudinal stress of concrete (unit: N/mm^2)

Fig.9 (a) shows the loads of outer RC component and inner CFST component versus axial strain (ε) relations. It can be seen that while the whole composite column reaches its ultimate strength, the outer RC component has reached the ultimate strength. The strength of CFST component does not decrease in the whole loading procedure. The strength of CFST component at the strain (ε_{scy}) is defined as the ultimate strength, where ε_{scy} is suggested by Han et al. (2005) to calculate the ultimate strength of circular CFST stub columns under axial compression. The strain (ε_{scy}) can be given as:

$$\varepsilon_{scy} = 1300 + 12.5 f_c^{'} + (600 + 33.5 f_c^{'}) \xi^{0.2} (\mu\varepsilon) \tag{2}$$

It can be seen that, in general, the CFST component in concrete-encased CFST approaches to the ultimate strength corresponding to Eq.(2).

Fig.9 (b) shows N_{cfst}/N_{cecfst} versus axial strain (ε) curve of the concrete-encased CFST column, where N_{cfst} and N_{cecfst} are the strength of inner CFST component and the whole concrete-encased CFST column, respectively. It can be found that, N_{cfst}/N_{cecfst} is about 0.3 before Point A. From Point A, the value of N_{cfst}/N_{cecfst} begins to increase slowly and it is 0.38 at Point C. After Point C, the increasing velocity of N_{cfst}/N_{cecfst} begins bigger. This contributes to the fact that the contribution of outer concrete decreases quickly after Point C, while the strength of the core concrete in CFST does not decrease due to the confinement of steel tube. The value of N_{cfst}/N_{cecfst} is 0.6 at Point D, and after that it does not change obviously significantly. It is obvious that at this stage, the CFST inside the composite column bears the majority of the applied axial load.

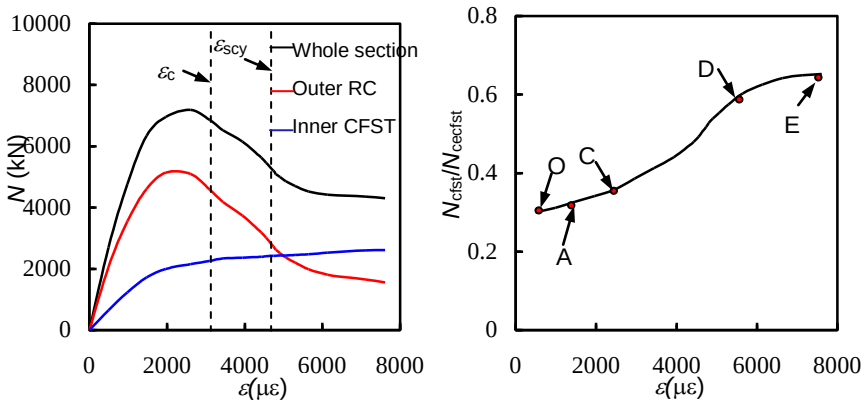

(a) N versus axial strain (ε) (b) N_{cfst}/N_{cecfst} versus axial strain (ε)

Fig. 9 Contributions of the CFST component and its outer RC component

4. Conclusions

Based on the limited results of this study, the following conclusions can be drawn:

(1) A finite element analysis (FEA) modeling of concrete-encased CFST stub columns with square section under axial compression is developed. Three different kinds of concrete are considered (i.e. concrete in CFST, outer confined concrete and

outer unconfined concrete). Generally good agreement is obtained between the predicted and measured results.

(2) The load (N) versus axial strain (ε) curve of the concrete-encased CFST column can be divided generally into five stages. When the whole composite column reaches its ultimate strength, the outer RC component has reached the ultimate strength. Though the strength of CFST component does not decrease in the whole loading procedure, it approaches to the ultimate strength at the peak load of the composite column.

(3) The outer RC component bears the majority of the applied axial load before peak load, while after that the inner CFST component bears the majority of the applied load.

Acknowledgements

The research reported in the paper is part of the Projects supported by Specialized Research Fund for the Doctoral Program of Higher Education (SRFDP) (20110002110017). The research is also supported by Tsinghua University Initiative Scientific Research Program (No. 2011THZ03). The financial support is highly appreciated.

References

ACI 318-11 (2011), *Building code requirements for structural concrete and commentary*. Detroit (USA): American Concrete Institute.

Attard, M.M. and Setunge, S. (1996), "Stress-strain relationship of confined and unconfined concrete." *ACI Mater. J.*, 93(5), 432-442.

Chen, Z.Y. (2002), "Study of the method for design and calculation of HSC columns reinforced with concrete filled steel tube." PhD Dissertations, Dalian University of Technology, Dalian [in Chinese].

Ellobody, E. and Young, B. (2011), "Numerical simulation of concrete encased steel composite columns." *J. Constr. Steel Res.*, 67(2), 211-222.

Han, L.H., Yao, G.H. and Tao, Z. (2007), "Performance of concrete-filled thin-walled steel tubes under pure torsion." *Thin-Walled Struct.*, 45(1), 24-36.

Han, L.H., Yao, G.H. and Zhao, X.L. (2005), "Tests and calculations for hollow structural steel (HSS) stub columns filled with self-consolidating concrete (SCC)." *J. Constr. Steel Res.,* 61(9), 1241-1269.

Han, L.H., Liao, F.Y., Tao, Z. and Hong, Z. (2009), "Performance of concrete filled steel tube reinforced concrete columns subjected to cyclic bending." *J. Constr. Steel Res.*, 65(8-9), 1607-1616.

Hibbitt, Karlson, Sorenson Inc. (2005), *ABAQUS Version 6.5: theory manual, users' manual, verification manual and example problems manua*l. Habbitt, Karlson and Sorenson Inc.

Hillerborg, A., Modéer, M. and Petersson, P.E. (1976), "Analysis of crack formation and crack growth in concrete by means of fracture mechanics and finite elements." *Cem. Concr. Res.,* 6(6),773–82.

Hoshikuma, J., Kawashima, K., Nagaya, K. and Taylor, A.W. (1997), “Stress-strain model for confined reinforced concrete in bridge piers.” *J. Struct. Eng., ASCE*, 123(5),624-633.

Huang, H., Han, L.H., Tao, Z. and Zhao, X.L. (2010),”Analytical behavior of concrete-filled double skin steel tubular (CFDST) stub columns.” *J. Constr. Steel Res.*, 66(4), 542-555.

Kang, H.Z. (2009), ”Study on mechanical properties of concrete-filled steel tube composite columns.” PhD Dissertations, Tsinghua University, Beijing, China [in Chinese].

Li, Y.J., Ren, Q.X. and Liao, F.Y. (2012),”Behavior of concrete filled steel tube reinforced concrete (CFSTRC) stub columns: experiments.” 2nd International Conference on Civil Engineering Architecture and Building Materials (CEABM 2012 Advances in Structures), Yan Tai.

Liu, L.Y. (2013), “Study on behavior of a new concrete-filled steel tube reinforced concrete column under axial compression.” Master Dissertations, Fuzhou University, Fuzhou, China [in Chinese].

Nie, J.G., Bai, Y. and Cai, C.S. (2008), “New connection system for confined concrete columns and beams. I: Experimental study.” *J. Struct. Eng., ASCE*, 134(12),1787-1799.

Papanikolaou, V.K. and Kappos, A.J. (2009), “Numerical study of confinement effectiveness in solid and hollow reinforced concrete bridge piers: Methodology.” *Comput. Struct.*, 87(21-22), 1427-1439.

Popovics, S. (1973), “A numerical approach to the complete stress-strain curve of concrete.” *Cem. Concr. Res.*, 3(5),583–599.

Sheikh, S.A. and Uzumeri, S.M. (1982), “Analytical model for concrete confinement in tied columns.” *J. Struct. Div.*, 1982, 108(12),2703-2722.

Zhao, X.M., Wu, Y.F. and Leung, A.Y.T. (2012), ”Analysis of plastic hinge regions in reinforced concrete beams under monotonic loading.” *Eng. Struct.*, 34,466-482.